Hybrid Precoding for mm-Wave Massive MIMO System

[1]*Naresh Purohit*, [2]*Lalit Bhanwrela*, [3]*Alka Karketta*,[4]*Kusum Tilkar*
[1,2,3] *Department of Electrical and Electronics Engineering, SVITS-SVVV, Indore, Madhya Pradesh, India*
[4] *Department of Computer Science Engineering, SVIIT-SVVV, Indore, Madhya Pradesh, India*

ABSTRACT
The evolving disruptive technologies such as massive machine-type communications, massive IoT, and vehicle-to-everything (V2X) give rise to challenges on the system of connectivity. They require massive machine connectivity, high reliability, enhanced mobile broadband, extended coverage, and diverse application requirements for the 5G network. Hybrid analog/digital precoding has emerged as a potential solution for carrying out the spatial multiplexing and multiuser transmission in millimeter wave (mm-Wave) massive MIMO (multiple-input multiple-output) systems. This work will be the opportunity to implement hybrid precoding architecture in the 5G cellular networks. In this work, we propose a hybrid precoder and combiner design in mm-wave communication with massive MIMO system considering both scenarios of perfect and imperfect channel state information (CSI). The capacity analysis of conventional fully digital precoding and hybrid precoding system is carried out at low and high SNR ranges for different channel setups. In experimental results, we found that the proposed design facilitates the 5G mm-Wave network and provides better system capacity compared with the existing design. Also, the result outcomes show improved uplink sum-rate (SR) for MRC and ZF receivers with perfect channel scenario and CSI uncertainty condition.

Keywords: 5G; capacity; hybrid precoding; massive MIMO; mm-Wave

1. INTRODUCTION

Millimeter Wave (mm-Wave) communication has emerged as one of the key new physical layer technology for 5G due to its very high carrier frequency and large bandwidth than the current cellular network[1, 2]. As the 5G in mobile connectivity, the cellular network will provide significantly higher data rates, lower latency, and the massive internet of things (IoT)[3–5]. Signal transmissions at mm-Wave bands (30 GHz -300 GHz) undergo higher propagation loss and penetration loss as compared to sub-6 GHz bands[6–8]. Owing to the smaller wavelength of mm-Wave bands, more antennas can be packed within the same physical dimension at both transmitter and receiver ends[9, 10]. The use of massive MIMO[11–13] within 5G network enhances energy efficiency, spectral efficiency, and individual user tracking capability of the system. In sub-6 GHz applications, implementation of the fully digital transceiver is feasible, and it utilizes the dedicated analog to digital converters (ADCs) and radio frequency (RF) chains[14]. For mm-Wave massive MIMO (multiple-input multiple-output) system, the implementation of the conventional fully digital transceiver is very difficult due to the costly hardware and a large amount of power consumption of RF chains[15]. Both digital precoding and analog beamforming have some problems when extending to mm-Wave band[16, 17]. To resolve this issue, hybrid precoding is proposed in mm-Wave massive MIMO systems. In this work, we develop strategies for hybrid precoder and combiner design in massive MIMO systems.

1.1. Related Literature

Zhang et al. [18] have proposed the idea of a soft antenna selection approach using hybrid analog/digital precoding in a MIMO system. The authors have described two transmission strategies named diversity and spatial multiplexing strategies. In results, they demonstrated the performance improvement of phase-shift and selection over hybrid selection scheme. Kim et al. [19] have described a hybrid beamforming scheme for mm-Wave channel, then formulates the RF beamformer and baseband precoder design problem that maximizing the link-level performance in terms of minimizing error probability. Ayach et al.[20] have presented a

hybrid analog/digital solution for sparse mm-Wave channels. The authors developed the precoder and combiner for single user massive MIMO system and utilize the basis pursuit algorithm. Rusu et al. [21] have described low complexity schemes to compute the design of hybrid precoder for single user and narrowband channel. The authors observed that with use of limited data stream and equal power allocation improves the achievable spectral efficiency for mm-Wave MIMO system. Adhikary et al. [22] have described an implementation of joint spatial division and multiplexing algorithm to realistic mm-Wave propagation channels. They concluded that proposed algorithms with good user selection improved the network Key Performance Indicators (KPIs). Stirling-Gallacher and Rahman [23] have proposed multi-user MIMO beamforming techniques for mm-Wave communication systems. The authors discussed codebook-based RF beamformer and non-code book based digital precoder. In the results, the authors show multi-user MIMO capacity improvement for indoor mm-Wave system operating at 60 GHz have 19 clusters. Cheng et al. [24] have developed a beamforming codebook design for the mm-Wave OFDM system operating at 60 GHz. The authors demonstrated the implementation of the time domain and frequency domain approach in compressive sensing-based scheme with the aim of improving the spectral efficiency of the system. Nguyen et al. [25] have proposed weighted minimum mean-squared error (WMMSE) hybrid precoder and combiner for mm-Wave multiuser system. The presented designs assume finite codebook-based RF beamformer at both the transmitter and receiver and sparse mm-Wave channel. Further, authors implemented compressed-sensing based algorithm to determine the hybrid precoder and combiner. Chopra and Kakkar [26] have discussed 5G mm-Wave heterogeneous networks and implemented the MMSE hybrid precoder and combiner. They concluded that selecting the appropriate value of channel gain of mm-Wave communication improves the capacity of the 5G network.

1.2. Contribution

This paper yields new conclusions on the implementation of optimal hybrid precoder and combiner in the sparse mm-Wave channel which can be summarized as:

- A study and mathematical analysis on massive MIMO systems and their significance in hybrid analog/digital precoding and combining.
- The comparative performance analysis between maximum-ratio combining (MRC) and zero-forcing (ZF) receiver, in terms of the uplink sum-rate (SR) performance with perfect channel scenario and CSI uncertainty condition.
- A novel comparative analysis on conventional MIMO and hybrid MIMO, in terms of the capacity (b/s/Hz) for different SNR ranges under specified channel setup.

1.3. Outline

Section 2 of the paper discusses on system model of massive MIMO under perfect CSI and CSI uncertainty conditions. mm-Wave massive MIMO systems are described in Section 3. Proposed procedure and analysis to determine the hybrid precoder and combiner are described in Section 4. Experimental setup and results are presented in Section 5. The work is concluded in Section 6.

2. MASSIVE MIMO SYSTEM

We consider the uplink of a massive MIMO system under perfect channel scenario and CSI uncertainty condition. The uplink system comprises one base station (BS) and K user equipment (UE) and here it is implemented with M antennas and a single antenna, respectively. The $(M \times 1)$ received vector y at the BS described in Ngo et al. [27] can be represented as (1)

$$y = \sqrt{p_u} \sum_{k=1}^{K} h_k x_k + n \tag{1}$$

$$= \sqrt{p_u} Hx + n \tag{2}$$

where $\sqrt{p_u}x$ is the transmitted symbols, H represents the channel matrix of size $(M \times K)$, and n denotes the $(M \times 1)$ additive noise vector.

The received signal for k_{th} UE in terms of desired signal and interference can be represented as (3)

$$y = \underbrace{\sqrt{p_u} h_k x_k}_{desired\ signal} + \underbrace{\sqrt{p_u} \sum_{k' \neq k}^{K} h_{k'} x_{k'}}_{interference} + \underbrace{n}_{noise} \tag{3}$$

2.1. SINR Analysis with perfect CSI

In perfect channel condition, the BS knows the perfect channel state information (CSI) i.e., channel matrix H. The received vector after the matched filter receiver or maximal ratio combiner for k_{th} UE can be expressed as (4)

$$r_k = \frac{h_k^H}{\|h_k\|} y \tag{4}$$

$$= \frac{h_k^H}{\|h_k\|} \left(h_k x_k + \sqrt{p_u} \sum_{k' \neq k}^{K} h_{k'} x_{k'} + n \right) \tag{5}$$

$$= \sqrt{p_u} \|h_k\| x_k + \sqrt{p_u} \sum_{k' \neq k}^{K} \frac{h_k^H}{\|h_k\|} h_{k'} x_{k'} + \frac{h_k^H}{\|h_k\|} n \tag{6}$$

where h_k and x_k are the k_{th} columns of the matrices H and x, respectively.

The received SINR of k_{th} UE can be represented as (7)

$$SINR = \frac{p_u \|h_k\|^2}{p_u \sum_{k' \neq k}^{K} E\left\{ \left| \frac{h_k^H}{\|h_k\|} h_{k'} \right|^2 \right\} + E\left\{ \left| \frac{h_k^H}{\|h_k\|} n \right|^2 \right\}} \tag{7}$$

The power of each UE is scaled with number of BS antenna M, as stated here $p_u = \frac{E_u}{M}$, then SINR stated in Nalband et al. [28], (7) can be reduced to expression (8),

$$SINR = E_u \beta_k = E_u \, E\left\{ \left| \frac{h_k^H}{\|h_k\|} h_{k'} \right|^2 \right\} \tag{8}$$

where β_k includes the intrinsic attenuation and small- scale scattering.

Referring to (8), this confirms that by using massive antenna array M at BS with perfect CSI, we can maintain constant SINR even with transmit power of each UE decreasing in proportion to 1/M.

2.2. SINR Analysis with CSI uncertainty

In imperfect channel condition, the BS estimates the channel matrix H. The channel estimate at the BS can be represented as (9)

$$\hat{H} = H + N \frac{1}{\sqrt{p_P}} \Phi^H = H + E \tag{9}$$

where the pilot matrix is considered as $\Phi\Phi^H = \mathrm{I}$, p_P is the pilot power, N represents the noise matrix with i.i.d. $\mathcal{CN}(0,1)$ and E denotes channel estimation error.

The received vector after matched filter receiver with CSI uncertainty for k_{th} UE can be represented as (10)

$$r_k = \hat{h}_k^H y \tag{10}$$

$$r_k = \sqrt{p_u}\|h_k\|^2 x_k + \sqrt{p_u} e_k^H h_k x_k + \sqrt{p_u} \sum_{i=1, i\neq k}^{K} \hat{h}_k^H h_i x_i + \hat{h}_k^H n \tag{11}$$

The received SINR of k_{th} UE can be expressed as (12)

$$SINR = \frac{p_u \|h_k\|^4}{p_u |e_k^H h_k|^2 + p_u \sum_{i=1, i\neq k}^{K} |\hat{h}_k^H h_i|^2 + E\left\{|\hat{h}_k^H n|^2\right\}} \tag{12}$$

Accordingly, $\hat{h}_k{}^H n \sim \mathcal{N}\left(0, \|\hat{h}_k\|^2\right)$ and $e_k^H \frac{h_k}{\|h_k\|} \sim \mathcal{N}(0, 1/Kp_u)$, also $\frac{\|h_k\|^2}{M} = \beta_k$ and $\frac{\|\hat{h}_k\|^2}{M} = (\beta_k + 1/Kp_u)$.

The power of each UE is scaled with number of BS antenna M, as stated here $p_u = \frac{E_u}{\sqrt{M}}$, then the SINR described in Nalband et al. [28], (12) can be reduced to expression (13),

$$SINR = K\beta_k{}^2 E_u{}^2 \tag{13}$$

3. mm-Wave MASSIVE MIMO SYSTEM

In mm-Wave massive MIMO system, signal processing is separated between baseband and RF section as shown in Fig. 1. This hybrid precoding allows spatial multiplexing and multi-user MIMO in the system, where the BS and UE accompanied by N_T and N_R antenna, respectively. The BS and UE have N_{RF} chain, where $N_{RF} \leq \min(N_T, N_R)$ and both communicate by means of N_s data stream. The transmitter applies an $(N_{RF} \times N_s)$ baseband precoder F_{BB} exploiting its N_{RF} chain subsequent by $(N_T \times N_{RF})$ RF precoder F_{RF}. Then, the received signal vector y can be represented as (14)

$$\tilde{y} = Hx + n = HF_{RF}F_{BB}s + n = HFs + n \tag{14}$$

where x is the transmitted signal, s denotes the $(N_S \times 1)$ signal vector and H represents the channel matrix of size $(N_R \times N_T)$.

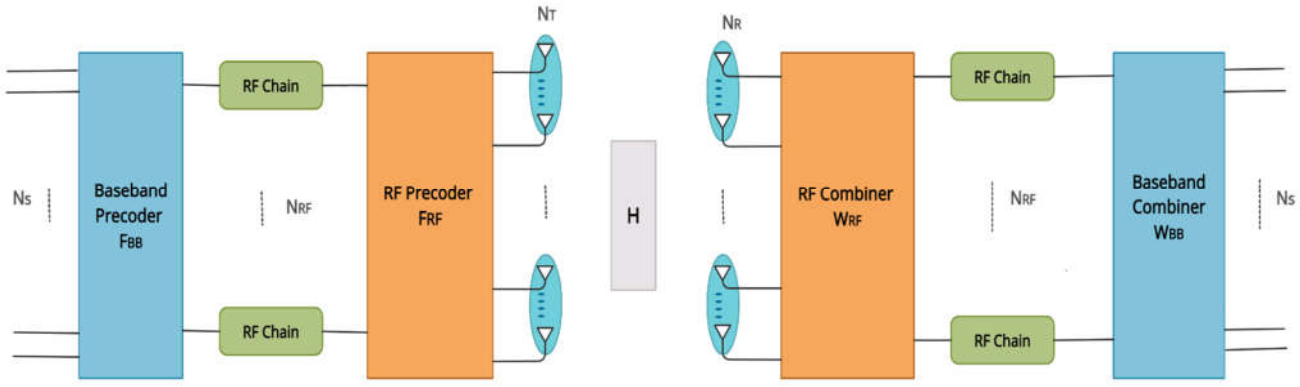

Fig. 1 Massive MIMO system at mm-Wave band with hybrid precoder and combiner

We consider the parametric channel model for mm-Wave massive MIMO system described in Lee et al. [29] with L scatters between BS and UE. The channel matrix H can be represented as (15)

$$H = \sum_{l=1}^{L} \alpha_l a_R(\theta_l^r)\, a_T^H(\theta_l^t) \tag{15}$$

where α_l denotes the complex gain and θ_l^r and θ_l^t represent the angle of arrival and angle of departure. $a_T(\theta_l^t)$ and $a_R(\theta_l^r)$ represent array response vectors at the BS and the UE, respectively. Considering transmitter and receiver configures the uniform linear arrays (ULA) and then $a_R(\theta_l^r)$ and $a_T(\theta_l^t)$ can be expressed as (16) and (17)

$$a_R(\theta_l^r) = \frac{1}{\sqrt{N_R}} \begin{bmatrix} 1 \\ e^{-j\frac{2\pi}{\lambda} d_r cos\theta_l^r} \\ \vdots \\ \vdots \\ e^{-j\frac{2\pi}{\lambda}(N_r-1) d_r cos\theta_l^r} \end{bmatrix} \tag{16}$$

$$a_T(\theta_l^t) = \frac{1}{\sqrt{N_T}} \begin{bmatrix} 1 \\ e^{-j\frac{2\pi}{\lambda} d_t cos\theta_l^t} \\ \vdots \\ \vdots \\ e^{-j\frac{2\pi}{\lambda}(N_t-1) d_t cos\theta_l^t} \end{bmatrix} \tag{17}$$

where λ represents the signal wavelength, d denotes the spacing between array elements and $e^{-j\frac{2\pi}{\lambda} d cos\theta}$ represents the phase difference between successive antenna elements.
Beamspace channel representation of channel model (15) can be expressed as (18)

$$H = A_R H_b A_T^H \tag{18}$$

where H_b denotes the sparse beamspace channel matrix and A_R and A_T represent the receive and transmit array response dictionary matrices, respectively. The channel estimation can be formulated as non-convex optimization problem as min $\|h_b\|_0$. This is termed as compressive sensing (CS). The non-convex optimization problem can be solved and implemented using CS based Orthogonal matching pursuit (OMP) algorithm.

4. mm-Wave MIMO HYBRID PRECODING

The hybrid precoding and combining would allow for highly directive transmission and reception of the desired signal in the mm-Wave massive MIMO system. Further, to receive desired signal at the receiver, the combiner $W = W_{RF} W_{BB}$ performs the reverse function of the transmitter (TX) precoder $F = F_{RF} F_{BB}$. Therefore, when precoding and combining operations are finished, the subsequent signal at the receiver is indicated by (19), where W_{BB} and W_{RF} represent the baseband combiner and RF combiner, respectively.

$$\tilde{y} = W_{BB}^H W_{RF}^H H F_{RF} F_{BB}\, s + W_{BB}^H W_{RF}^H\, n \tag{19}$$

The spectral efficiency of mm-Wave communication described in Ayach et al. [20], can be represented as (20)

$$R = log_2\left(\left| I_{N_s} + \frac{p}{N_s} R_n^{-1} W_{BB}^H W_{RF}^H H F_{RF} F_{BB} \times F_{BB}^H F_{RF}^H H^H W_{RF} W_{BB} \right|\right) \tag{20}$$

where $\mathrm{R_n} = \sigma_n^2 \mathrm{W_{BB}^H W_{RF}^H W_{RF} W_{BB}}$ represents the noise covariance matrix and p denotes average received signal power.

Accordingly, the main goal of mm-Wave MIMO precoder and combiner is to boost the spectral efficiency of system through suitable design of precoding matrices F_{BB}, F_{RF} and combining matrices W_{BB}, W_{RF} in effective manner.

Simultaneous design of mm-Wave MIMO precoding and combining is highly complex. Therefore, the scheme of designing precoders and combiners are split into parts. Specifically, let us initially design the precoder and then the combiner, and they both take the same approach in finding solutions. Hence, achievable mutual information can be expressed as (21)

$$\Gamma(F_{RF}, F_{BB}) = log_2\left(\left|\mathrm{I} + \frac{p}{N_s\sigma_n^2} H F_{RF} F_{BB} F_{BB}^H F_{RF}^H H^H\right|\right) \tag{21}$$

Accordingly, let us consider the optimal precoder as $F_{opt} = F_{RF}F_{BB}$. Hence, the design of best precoder problem can be formulated as (22)

$$\begin{aligned} &\arg\min_{A_T, \tilde{F}_{BB}} \left\{\left\| F_{opt} - A_T, \tilde{F}_{BB}\right\|_F\right\} \\ &\text{subject to } \left\|diag\left(\tilde{F}_{BB}\tilde{F}_{BB}^H\right)\right\|_0 = N_{RF}\ , \\ &\left\|A_T, \tilde{F}_{BB}\right\|_F^2 = N_S \end{aligned} \tag{22}$$

Further, the optimal minimum mean square error (MMSE) combiner can be obtained at the receiver (RX) as (23)

$$\bar{W}_{opt}^H = F_{BB}^H F_{RF}^H H^H \times (H F_{RF} F_{BB} F_{BB}^H F_{RF}^H H^H + N_s\sigma_n^2 \mathrm{I})^{-1} \tag{23}$$

The design of mm-Wave optimal combiner problem can be formulated as (24)

$$\arg\min_{A_R, \widetilde{W}_{BB}} \left\{\left\| R_{yy}^{1/2}(\bar{W}_{opt} - A_R, \widetilde{W}_{BB})\right\|_F\right\} \tag{24}$$

where $\mathrm{R_{yy}} = H F_{RF} F_{BB} F_{BB}^H F_{RF}^H H^H + N_s\sigma_n^2 \mathrm{I}$ denotes the combiner auto-correlation matrix.

As aforementioned, procedure to find best approximation to precoder and combiner are analogous, and therefore we only showing the OMP based design procedure of optimal precoder for transmitter in this work. Based on the above procedure, the design scheme of the proposed precoder as described in the algorithm is as follows.

Input: Precoder F_{opt} .

Output: Precoder F_{RF} and F_{BB}.

Step1: Initialize the RF precoder as the null matrix $F_{RF}^{(0)} = [\,]$.

Step2: Set initial residue as the optimal precoder $F_{res}^{(0)} = F_{opt}$.

Step3: Let iteration k= 1 .

Step4: Evaluate the maximum correlation of $F_{res}^{(k-1)}$ with transmit array response matrix A_T .

Compute $\Psi = A_T^H F_{res}^{(k-1)}$ and $i(k) = \arg\max\ [\Psi\Psi^H]_{l,l}$.

Step5: Augment the RF precoder matrix with $i(k)th$ column of transmit array response matrix.

Compute $F_{RF}^{(k)} = \left\{F_{RF}^{(k-1)} \middle| a_T(\theta_{i(k)})\right\}$.

Step6: Calculate the best approximation to baseband precoder.

Compute $F_{BB}^{(k)} = \left(\left(F_{RF}^{(k)}\right)^H F_{RF}^{(k)}\right)^{-1} \left(F_{RF}^{(k)}\right)^H F_{opt}$.

Step7: Calculate residue as $F_{res}^{(k)} = \frac{F_{opt} - F_{RF}^{(k)} F_{BB}^{(k)}}{\left\| F_{opt} - F_{RF}^{(k)} F_{BB}^{(k)}\right\|_F}$.

Step8: Set k= $k+1$; $if\ k \le N_{RF}$, go to Step4, otherwise stop the process.

We provide a computational approach built on the well-known idea of orthogonal matching pursuit. Algorithm contains the pseudo-code for the precoder solution. The transmit array response matrix A_T, along which the optimal precoder has the maximum projection, is found as the main step in the precoding procedure. A_T is then added to the RF precoder F_{RF} along with the chosen column transmit array response matrix. The least squares solution to the F_{BB} is calculated in step 6 after the dominant vector has been identified. Step 7 eliminates the contribution of the chosen vector, and the algorithm then searches for the column along which the residual matrix F_{res} has the most significant projection. The procedure is repeated up until the selection of all N_{RF} beamforming vectors.

Table 1 Simulation parameters

Parameter	Value
No. of TX Antennas	32
No. of RX Antennas	32
No. of RF Chains	6
Grid Size	64
Sparsity level	8
No. of data streams	6

5. SIMULATION RESULTS AND DICUSSION

To obtain further insight into the proposed hybrid precoder and combiner, we simulate massive MIMO system under perfect channel knowledge condition and CSI uncertainty scenario. The implementation of the proposed scheme has been simulated on MATLAB software under various parameter settings to demonstrate and validate its accuracy. Furthermore, we analyze the hybrid precoder performance in terms of system capacity by implementing the OMP based algorithm.

Fig. 2, Fig. 3, Fig. 4, and Fig. 5 illustrate the simulated uplink SR performance and proposed bounds for massive MIMO receivers at pilot transmit power 10dB. In this case, there are 10 UEs in the uplink system.

From Fig. 2, we can observe that as the number of BS antennas is varied from 0 to 500, the SR performance for perfect CSI of ZF (Zero Forcing) receiver is in the order of 12 to 68 bits/sec/Hz. In this case, the SR curve for MRC (Maximal Ratio combining) is changing from 10 to 40 bits/sec/Hz. We observed that SR performance per UE for ZF receiver and MRC are of 1 to 6 bits/sec/Hz and 1 to 4 bits/sec/Hz, respectively.

From Fig. 3, we can examine that as the number of BS antennas is varied as the above, the SR performance for perfect CSI with power scaling of ZF receiver is in the order of 2 to 5 bits/sec/Hz. In this case, the SR curve for MRC is changing from 4 to 5 bits/sec/Hz. We observed that when $p_u = \frac{E_u}{M}$, SR performance at the very large number of BS antenna M, these two lines coincide with one another.

According to Fig. 4, it is illustrated that as the number of BS antennas is varied from 0 to 500, the SR performance for imperfect CSI of ZF receiver is changing from 10 to 47 bits/sec/Hz. In this case, the SR curve for MRC is in the order of 8 to 31 bits/sec/Hz. Further, it can also be examined that the SR performance with imperfect CSI is lower than the perfect channel condition due to the presence of channel estimation error.

From Fig. 5, it is observed that as the number of BS antennas is varied as the above, the SR performance for imperfect CSI with power scaling of ZF receiver is in the order from 4 to 13 bits/sec/Hz. In this case, the SR curve for MRC is changing from 6 to 12 bits/sec/Hz. When comparing both the receivers in this scenario, we can see that when we apply $p_u = \frac{E_u}{M}$, the SR performance of ZF receiver and MRC approaches to zero as M increases. However, with $p_u = \frac{E_u}{\sqrt{M}}$, the SR performance consistent with finite values.

From Fig. 2, Fig. 3, Fig. 4, and Fig. 5, it is evident that SR performance of our proposed work is better than SR performance of existing work proposed in Nalband et al. [28] and Kumar et al. [30]. Overall, the ZF receiver performs better than MRC. Further, it can also be observed that for a power scaling scenario at the low value of M, the SR curve of MRC performs better than ZF. As the value of M increases to high numbers, ZF performance approaches very closely to MRC.

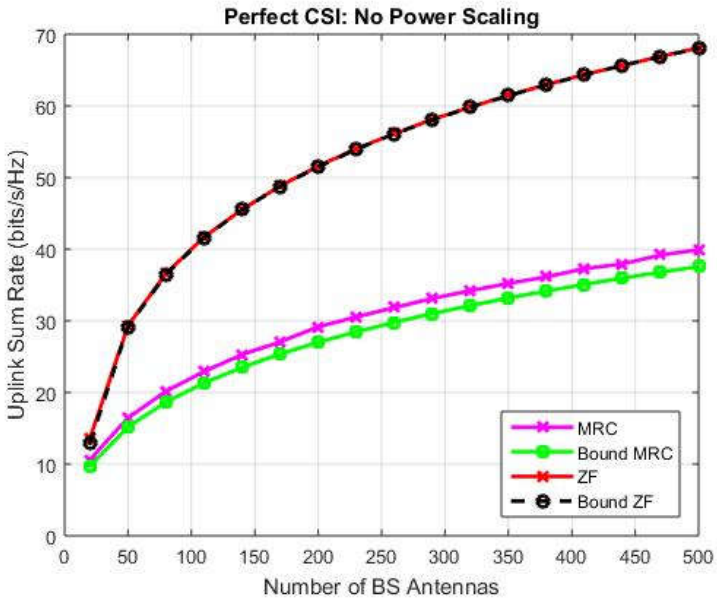

Fig. 2 Sum-rate (SR) vs No. of BS antennas for massive MIMO perfect CSI with no power scaling

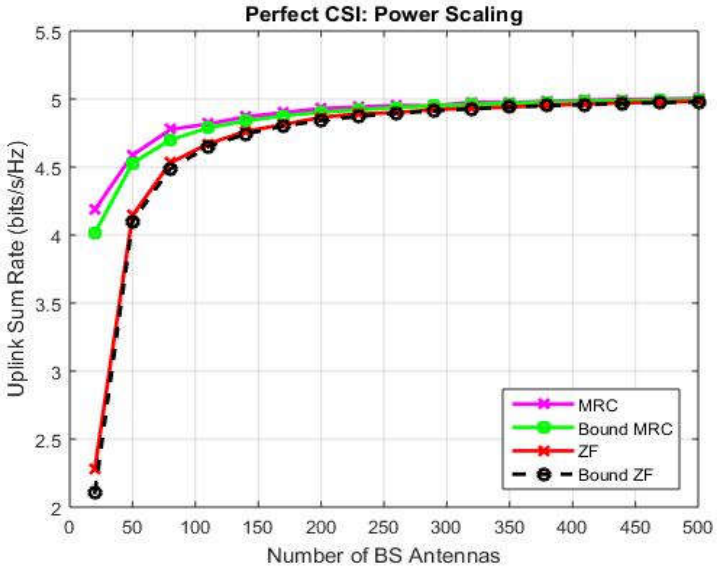

Fig. 3 Sum-rate (SR) vs No. of BS antennas for massive MIMO perfect CSI with power scaling

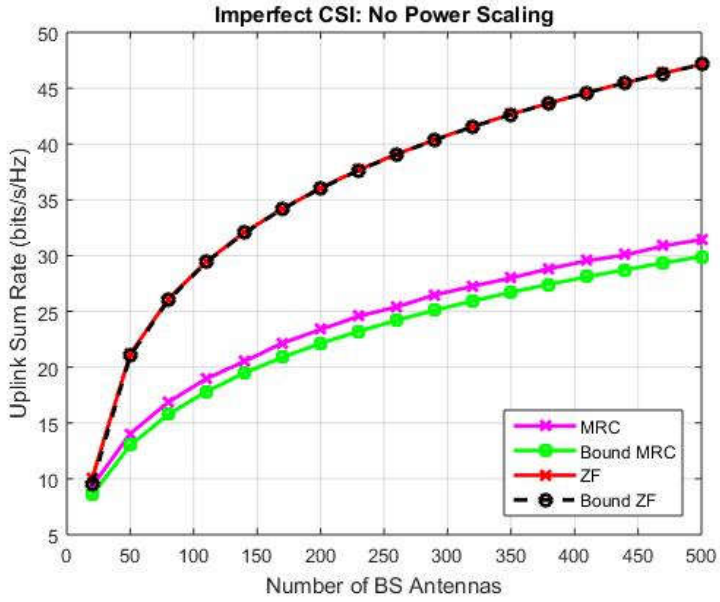

Fig. 4 Sum-rate (SR) vs No. of BS antennas for massive MIMO imperfect CSI with no power scaling

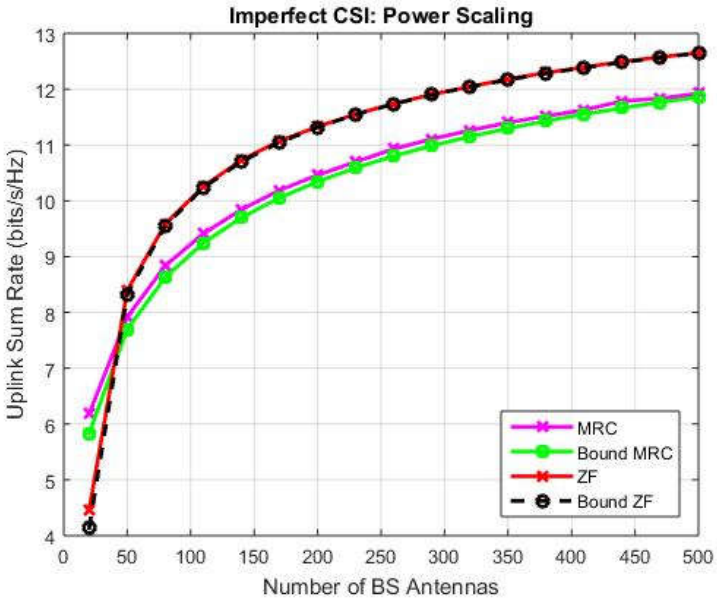

Fig. 5 Sum-rate (SR) vs No. of BS antennas for massive MIMO imperfect CSI with power scaling

The capacity of hybrid MIMO system or hybrid precoder is formulated in simulation as (25)

$$C_{hybrid(at\ given\ SNRdB)} = C(W_{BB}^{H} * W_{RF}^{H} * H * F_{RF} * F_{BB} * Normalized\ F_{BB},\ 1/N_S * I_{N_S} * noise\ power * W_{BB}^{H} * W_{RF}^{H} * W_{RF} * W_{BB}) \quad (25)$$

Fig. 6 and Fig. 7 illustrate the capacity versus SNR curves for our proposed hybrid precoding method. To analyze the system performance, we have considered two different types of SNR range. In the first case, SNRdB = -5:1:5 dB and second case SNRdB = -40:1:40 dB. The simulation parameters used in implementation are shown in Table 1**.** Further, the setup considered for implementation of our proposed work consist of $N_T = 32$, $N_R = 32$, $N_{RF} = 6$, $N_s = 6$, $G = 64$, and $L = 8$.

Fig. 6 shows the capacity versus received SNR curve for a scenario where SNRdB is varied from -5 to 5 dB. From the simulation result, it can be examined that the capacity curve of the hybrid precoder is in the order of 29 to 49 bits/sec/Hz.

Fig. 7 shows how the variation of received SNR affects the capacity of system in the sparse mm-Wave MIMO channel. In this case, SNRdB is varied from -40 to 40 dB. The simulation result is examined for the hybrid precoder and conventional MIMO system. From Fig. 7, it can be noticed that the capacity curve of hybrid precoder is in the order of 0 to 119 bits/sec/Hz.

From Fig. 6 and Fig. 7, it can be examined that the performance of the proposed hybrid precoder approaches very closely to conventional fully digital precoder which is used in sub-6 GHz communication. Further, it can also be observed that the capacity curve of proposed work is better than the capacity curve of the existing work suggested in Chopra and Kakkar [26] as part of the mentioned simulation parameter as described in Table 1.

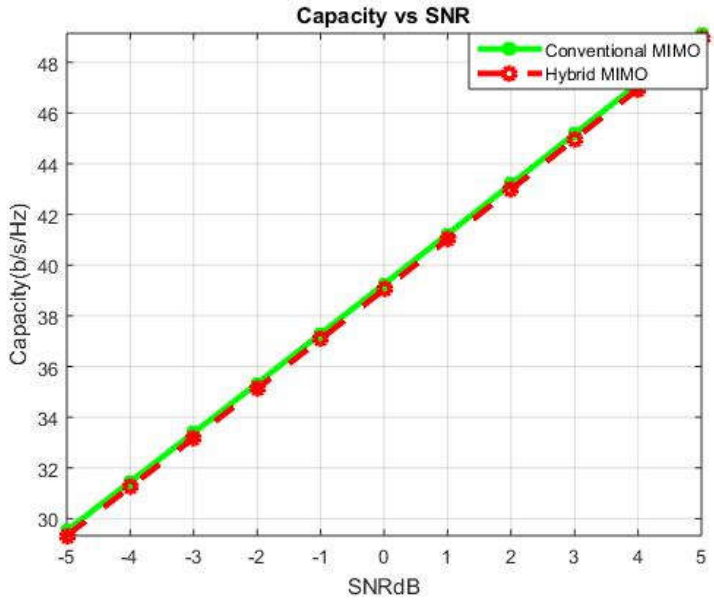

Fig. 6 Capacity vs received SNR for mm-Wave band at low SNR regime

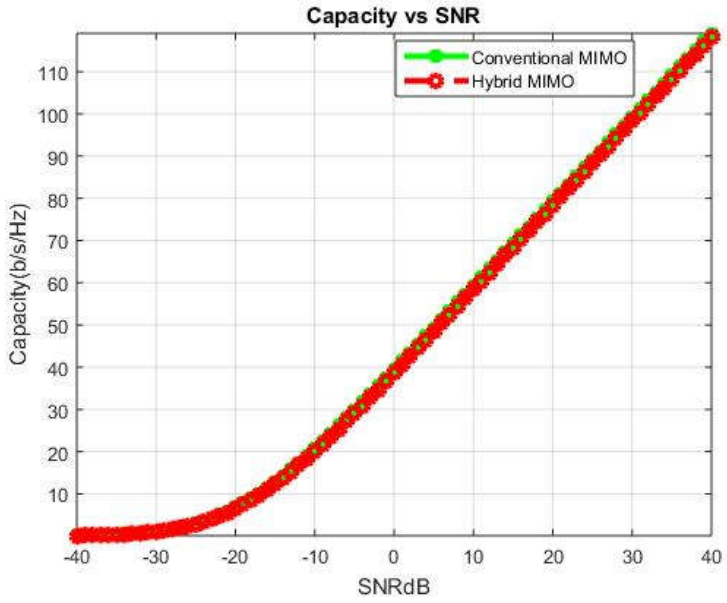

Fig. 7 Capacity vs received SNR for mm-Wave band at high SNR regime

6. CONCLUSIONS

This work investigated the performance of hybrid precoder and combiner under the framework of 5G mm-Wave massive MIMO system. Here, the proposed analysis has been implemented with perfect channel scenario and CSI uncertainty condition. The ZF receiver outperforms the MRC receiver in no power scaling scenarios. The proposed work is also analyzed for the power scaling scenario, and it is found that the SR curve of MRC outperforms the ZF curve for low numbers of BS antennas. When the number of BS antennas is significantly high, ZF performance approaches that of the MRC. Further, in consideration along with two

different types of SNR range and channel setup, the capacity of the hybrid precoding method is verified. According to the experimental outcome, the capacity range of the hybrid precoder is in the order of 0 to 119 bits/sec/Hz and 29 to 49 bits/sec/Hz for SNRdB range of -40 to 40 dB and -5 to 5 dB, respectively. In the analysis, we found that the performance of the proposed design approaches near-optimal to conventional fully digital precoder. For future directions, we suggest work focusing on multi-cell channel estimation and multi-cell power scaling under Rician fading channel in 5G mm-Wave massive MIMO system.

DECLARATIONS

Funding: No funding was received for conducting this study.

Conflicts of interest/Competing interests: The authors have no relevant financial or non-financial interests to disclose.

Availability of data and material: Data sharing not applicable to this article as no datasets were generated or analyzed during the current study.

Code availability: Custom code in MATLAB has been used for simulation.

References

1. Rappaport, T. S., Sun, S., Mayzus, R., Zhao, H., Azar, Y., Wang, K., Gutierrez, F. (2013). Millimeter wave mobile communications for 5G cellular: It will work! *IEEE Access*, *1*, 335–349. https://doi.org/10.1109/ACCESS.2013.2260813
2. Niu, Y., Li, Y., Jin, D., Su, L., & Vasilakos, A. V. (2015). A survey of millimeter wave communications (mmWave) for 5G : opportunities and challenges. *Wireless Networks*, *21*(8), 2657–2676. https://doi.org/10.1007/s11276-015-0942-z
3. Liu, G., & Jiang, D. (2016). 5G: Vision and Requirements for Mobile Communication System towards Year 2020. *Chinese Journal of Engineering*, *2016*(March 2016). https://doi.org/10.1155/2016/5974586
4. Sahoo, B. P. S., Chou, C. C., Weng, C. W., & Wei, H. Y. (2019). Enabling millimeter-wave 5g networks for massive IoT applications: A closer look at the issues impacting millimeter-waves in consumer devices under the 5g framework. *IEEE Consumer Electronics Magazine*, *8*(1), 49–54. https://doi.org/10.1109/MCE.2018.2868111
5. Siddiqi, Yu, Joung, J., Siddiqi, M. A., Yu, H., & Joung, J. (2019). 2019 5G Ultra-Reliable Low-Latency Communication.pdf. *Electronics*, *8*(9), 981. Retrieved from https://www.mdpi.com/2079-9292/8/9/981
6. Rappaport, T. S., Xing, Y., MacCartney, G. R., Molisch, A. F., Mellios, E., & Zhang, J. (2017). 6. mmWaver focus propagation. *IEEE Transactions on Antennas and Propagation*, *65*(12), 6213–6230.
7. Fuschini, F., Häfner, S., Zoli, M., Müller, R., Vitucci, E. M., Dupleich, D., Thomä, R. S. (2016). Item level characterization of mm-wave indoor propagation. *Eurasip Journal on Wireless Communications and Networking*, *2016*(1), 1–12. https://doi.org/10.1186/s13638-015-0502-3
8. Uwaechia, A. N., & Mahyuddin, N. M. (2020). A comprehensive survey on millimeter wave communications for fifth-generation wireless networks: Feasibility and challenges. *IEEE Access*, *8*, 62367–62414. https://doi.org/10.1109/ACCESS.2020.2984204
9. Wang, X., Kong, L., Kong, F., Qiu, F., Xia, M., Arnon, S., & Chen, G. (2018). Millimeter wave communication: A comprehensive survey. *IEEE Communications Surveys and Tutorials*, *20*(3), 1616–1653. https://doi.org/10.1109/COMST.2018.2844322
10. Hemadeh, I. A., Satyanarayana, K., El-Hajjar, M., & Hanzo, L. (2018). Millimeter-Wave Communications: Physical Channel Models, Design Considerations, Antenna Constructions, and Link-Budget. *IEEE Communications Surveys and Tutorials*, *20*(2), 870–913. https://doi.org/10.1109/COMST.2017.2783541
11. Busari, S. A., Huq, K. M. S., Mumtaz, S., Dai, L., & Rodriguez, J. (2018). Millimeter-Wave Massive MIMO Communication for Future Wireless Systems: A Survey. *IEEE Communications Surveys and Tutorials*, *20*(2), 836–869. https://doi.org/10.1109/COMST.2017.2787460
12. Chataut, R., & Akl, R. (2020). Massive MIMO systems for 5G and beyond networks—overview, recent trends, challenges, and future research direction. *Sensors (Switzerland)*, *20*(10), 1–35. https://doi.org/10.3390/s20102753
13. A. Lee Swindlehurst, Ender Ayanoglu, Payam Heydari, & and Filippo Capolino. (2014). Millimeter-Wave Massive MIMO: The Next Wireless Revolution? *IEEE Communications Magazine*, *52*(9), 56–62.
14. Heath, R. W., Gonzalez-Prelcic, N., Rangan, S., Roh, W., & Sayeed, A. M. (2016). An Overview of Signal Processing Techniques for Millimeter Wave MIMO Systems. *IEEE Journal on Selected Topics in Signal Processing*, *10*(3), 436–453. https://doi.org/10.1109/JSTSP.2016.2523924

15. Han, S., I, C. L., Xu, Z., & Rowell, C. (2015). Large-scale antenna systems with hybrid analog and digital beamforming for millimeter wave 5G. *IEEE Communications Magazine*, *53*(1), 186–194. https://doi.org/10.1109/MCOM.2015.7010533
16. Zhao, L., Ng, D. W. K., & Yuan, J. (2017). Multi-User Precoding and Channel Estimation for Hybrid Millimeter Wave Systems. *IEEE Journal on Selected Areas in Communications*, *35*(7), 1576–1590. https://doi.org/10.1109/JSAC.2017.2699378
17. Ahmed, I., Khammari, H., Shahid, A., Musa, A., Kim, K. S., De Poorter, E., & Moerman, I. (2018). A survey on hybrid beamforming techniques in 5G: Architecture and system model perspectives. *IEEE Communications Surveys and Tutorials*, *20*(4), 3060–3097. https://doi.org/10.1109/COMST.2018.2843719
18. Zhang, X., Molisch, A. F., & Kung, S. Y. (2005). Variable-phase-shift-based RF-baseband codesign for MIMO antenna selection. *IEEE Transactions on Signal Processing*, *53*(11), 4091–4103. https://doi.org/10.1109/TSP.2005.857024
19. Kim, T., Park, J., Seol, J., Jeong, S., Cho, J., & Roh, W. (2013). 06831646 Tens of Gbps Support with mmWave Beamforming Systems for Next Generation Communications by Samsung in Globe comm 2013.pdf (pp. 3685–3690).
20. Ayach, O. El, Rajagopal, S., Abu-Surra, S., Pi, Z., & Heath, R. W. (2014). Spatially sparse precoding in millimeter wave MIMO systems. *IEEE Transactions on Wireless Communications*, *13*(3), 1499–1513. https://doi.org/10.1109/TWC.2014.011714.130846
21. Rusu, C., Mendez-Rial, R., Gonzalez-Prelcic, N., & Heath, R. W. (2016). Low Complexity Hybrid Precoding Strategies for Millimeter Wave Communication Systems. *IEEE Transactions on Wireless Communications*, *15*(12), 8380–8393. https://doi.org/10.1109/TWC.2016.2614495
22. Adhikary, A., Al Safadi, E., Samimi, M. K., Wang, R., Caire, G., Rappaport, T. S., & Molisch, A. F. (2014). Joint spatial division and multiplexing for mm-Wave channels. *IEEE Journal on Selected Areas in Communications*, *32*(6), 1239–1255. https://doi.org/10.1109/JSAC.2014.2328173
23. Stirling-Gallacher, R. A., & Rahman, M. S. (2015). Multi-user MIMO strategies for a millimeter wave communication system using hybrid beam-forming. In *IEEE International Conference on Communications* (Vol. 2015-Septe, pp. 2437–2443). https://doi.org/10.1109/ICC.2015.7248690
24. Cheng, X., Wang, M., & Li, S. (2017). Compressive Sensing-Based Beamforming for Millimeter-Wave OFDM Systems. *IEEE Transactions on Communications*, *65*(1), 371–386. https://doi.org/10.1109/TCOMM.2016.2616390
25. Nguyen, D. H. N., Le, L. B., Le-Ngoc, T., & Heath, R. W. (2017). Hybrid MMSE Precoding and Combining Designs for mmWave Multiuser Systems. *IEEE Access*, *5*, 19167–19181. https://doi.org/10.1109/ACCESS.2017.2754979
26. Chopra, S., & Kakkar, A. (2021). Capacity Analysis of Hybrid MIMO Using Sparse Signal Processing in mmW 5G Heterogeneous Wireless Networks. *Wireless Personal Communications*, *116*(3), 2651–2673. https://doi.org/10.1007/s11277-020-07815-z
27. Ngo, H. Q., Larsson, E. G., & Marzetta, T. L. (2013). Energy and spectral efficiency of very large multiuser MIMO systems. *IEEE Transactions on Communications*, *61*(4), 1436–1449. https://doi.org/10.1109/TCOMM.2013.020413.110848
28. Nalband, A. H., Sarvagya, M., & Ahmed, M. R. (2020). Optimal Hybrid Precoding for Millimeter wave Massive MIMO Systems. *Procedia Computer Science*, *171*(2019), 810–819. https://doi.org/10.1016/j.procs.2020.04.088
29. Lee, J., Gil, G. T., & Lee, Y. H. (2016). Channel Estimation via Orthogonal Matching Pursuit for Hybrid MIMO Systems in Millimeter Wave Communications. *IEEE Transactions on Communications*, *64*(6), 2370–2386. https://doi.org/10.1109/TCOMM.2016.2557791
30. Kumar, I., Sachan, V., Shankar, R., & Mishra, R. K. (2020). Performance Analysis of Multi-User Massive MIMO Systems with Perfect and Imperfect CSI. *Procedia Computer Science*, *167*(2019), 1452–1461. https://doi.org/10.1016/j.procs.2020.03.356